Talanta 128 (2014) 311–318

Contents lists available at ScienceDirect

Talanta

journal homepage: www.elsevier.com/locate/talanta

# Facile synthesis of multifunctional multi-walled carbon nanotube for pathogen *Vibrio alginolyticus* detection in fishery and environmental samples

Yue Liu [a,*], Jia Hu [b], Jin-Sheng Sun [c], Yan Li [d], Shu-Xia Xue [c], Xiao-Qin Chen [e], Xiao-Shuang Li [a], Gui-Xiang Du [a]

[a] Tianjin Key Laboratory of Structure and Performance for Functional Molecules, Key Laboratory of Inorganic–Organic Hybrid Functional Material Chemistry, Ministry of Education, College of Chemistry, Tianjin Normal University, Tianjin 300387, China
[b] Beijing Guodian Futong Science and Technology Development Co., Ltd., Beijing 102401, China
[c] Tianjin Center for Control and Prevention of Aquatic Animal Infectious Disease, Tianjin Fishery Institute, Tianjin 300221, China
[d] Department of Chemistry, Nankai University, Tianjin 300071, China
[e] Tianjin Guangfu Fine Chemical Research Institute, Tianjin 300384, China

ARTICLE INFO

*Article history:*
Received 20 December 2013
Received in revised form
9 April 2014
Accepted 12 April 2014
Available online 29 April 2014

*Keywords:*
Multi-walled carbon nanotubes
*Vibrio alginolyticus* (Va)
Immuno-magnetic-fluorescent sensor
Ultrasensitive detection

ABSTRACT

Interest in carbon nanotubes for detecting the presence of pathogens arises because of developments in chemical vapor deposition synthesis and progresses in biomolecular modification. Here we reported the facile synthesis of multi-walled carbon nanotubes (MWCNTs), which functioned as immuno-, magnetic, fluorescent sensors in detecting *Vibrio alginolyticus* (Va). The structures and properties of functionalized MWCNTs were characterized by ultraviolet (UV), Fourier transform infrared spectra (FT-IR), X-ray diffraction (XRD), vibrating sample magnetometer (VSM), magnetic property measurement system (MPMS) and fluorescent spectra (FL). It was found that the functionalized MWCNTs showed: (1) low nonspecific adsorption for antibody–antigen, (2) strong interaction with antibody, and (3) high immune-magnetic activity for pathogenic cells. Further investigations revealed a strong positive linear relationship ($R=0.9912$) between the fluorescence intensity and the concentration of Va in the range of $9.0\times10^2$ to $1.5\times10^6$ cfu mL$^{-1}$. Moreover, the relative standard deviation for 11 replicate detections of $1.0\times10^4$ cfu mL$^{-1}$ Va was 2.4%, and no cross-reaction with the other four strains was found, indicating a good specificity for Va detection. These results demonstrated the remarkable advantages of the multi-functional MWCNTs, which offer great potential for the rapid, sensitive and quantitative detection of Va in fishery and environmental samples.



## 1. Introduction

*Vibrio alginolyticus* (Va) is a Gram-negative straight rod marine bacterium. It shows severe hazardous to aquatic animals such as fish, shrimp and shellfish. Intake of Va contaminated seafood or water also cause acute diarrhea even at very low concentration [1–4]. Va infections not only pose a serious threat to human health, but also cause widespread damage [5]. However, bacteria at low concentrations are hard to detect and usually require long induction times before further analysis. Currently, identification and quantification of Va are generally based on the polymerase chain reaction (PCR) and enzyme-linked immunosorbent assay (ELISA). Though PCR provides high sensitivity, it requires precise and expensive instruments. ELISA shows good specificity, sound sensitivity and low cost, but it is time-consuming and tends to result in false-positive signals because of nonspecific surface interactions. Therefore developing rapid and sensitive method for detecting Va is greatly needed.

Carbon nanotubes (CNTs) are composed of one-dimensional cylindrical nanostructure. CNTs have attracted intensive attention from chemists and biologists because of their physical properties, including low density, high electrical conductivity, considerable

*Abbreviations:* MWCNTs, multi-walled carbon nanotubes; Va, *Vibrio alginolyticus*; UV, ultraviolet; FT-IR, Fourier transform infrared spectra; XRD, X-ray diffraction; FL, fluorescent spectra; PCR, polymerase chain reaction; ELISA, enzyme-linked immunosorbent assay; CNTs, Carbon nanotubes; *E. coli*, *Escherichia coli*; *S. aureus*, *Staphyloccocus aureus*; *B. subtilis*, *Bacillus subtilis*; *S. mutans*, *Streptococcus mutans*; *L. pneumophila*, *Legionella pneumophila*; Va-Ab, specific Va antibodies; py, 1-pyrenebutyric acid; MWCNTs-COOH, oxidized MWCNTs; $Et_3N$, triethylamine; DMF, *N, N*-dimethylformamide; NHS, *N*-hydroxysuccinimide; DCC, 1,3-dicyclohexyl-carbo-diimide; PBS, phosphate-buffered saline; MES, 2-(4-morpholino)ethanesul-fonic acid; SEM, scanning electron microscopy; VSM, vibrating sample magnetometer; Ms, saturation magnetization; MPMS, magnetic property mea-surement system; $ddH_2O$, double distilled water

* Corresponding author.
*E-mail address:* nkcmliu@yahoo.com (Y. Liu).

http://dx.doi.org/10.1016/j.talanta.2014.04.048
0039-9140/

porosity, and specific surface area *etc*. [6,7]. Thus, CNTs are considered as promising materials for hydrogen storage, catalyst support, and chemical sensors especially in life sciences [8–10]. For these applications, the protein bioactivity and stability, which is the major concern, are well remained by protein-binding to CNT surface [11–13]. Therefore CNTs have been viewed as the suitable vectors for protein delivery and recognition *in vitro* and *in vivo* [14,15], solid-phase extraction for isolating proteins [16] and cancer biomarkers [17].

Recently, many efforts have been made to futher explore the ability of CNTs as bacterial filter or sensors. CNTs have been proved to be a good absorbent for many bacteria with different sizes and shapes, such as *Escherichia coli* (*E. coli*), *Staphyloccocus aureus* (*S. aureus*), *Bacillus subtilis* (*B. subtilis*), *Streptococcus mutans* (*S. mutans*) and *Legionella pneumophila* (*L. pneumophila*) [18–23]. Gutierrez's group also found that multi-walled carbon nanotube (MWCNT) scaffold exhibits remarkable biocompatibility for *E. coli*, which allows for bacteria immobilization and proliferation within its micro-channel structure [24]. The biomolecule-CNT composites have novel mechanical, biological, optical, electronic and magnetic properties. They have been continually explored for the potential applications in various fields including molecular electronics, medical chemistry, and biomedical engineering [25]. In order to further enhance the efficiency of bacteria purification, several bio-separation strategies have been delicately applied for capturing bacteria. Magnetic bio-separation is one of the kind [26,27]. Immuno-MWCNTs functionalized with ferromagnetic metal particles display good separation for *E. Coli O157:H7* [28], and the magnetic susceptibility and high bacterial affinity of CNT clusters suggest their good potential as reagent for magnetic bio-separation platform [29,30].

However, those functionalized CNTs exhibit unsatisfactory specificity toward certain bacterium species and yet have not achieved quantitative analysis in complicated matrices by optical density. Usually ELISA is well adopted to quantitatively monitor the Va density. Because of its complicated protocol, the sensitivity of ELISA color reaction is often compromised, thus failed to detect Va in low density. Although the sensitivity of ELISA can be improved by green fluorescent protein labeling technology, the cost is highly increased and the protocol becomes more complicated, which makes it less suitable for rapid analysis.

Here, we design a multi-functional MWCNTs based method to achieve rapid, sensitive and specific detection of Va. Three major modifications were made. First, in order to obtain highly specific interaction with the target bacteria Va, antibody (Va-Ab) was adopted. Thus selective separating and further preconcentrating of Va was possible. Second, fluorescent reagent 1-pyrenebutyric acid (py) was used to construct the report system. Py showed advantages in two major aspects. On one hand, the changes of the fluorescence intensity, as far as observed in this study, was linearly related to the bacteria density. So the quantitative detection of Va is possible [31]. On the other hand, the aromatic structure of py molecule stabilized its conjugation to MWCNTs sidewall *via* strong π–π stacking interaction. Also py facilitated the Va-Ab's binding toward MWCNTs [32]. Lastly, the MWCNTs scaffold were futher grafted by poly(ethylene glycol) (PEG) which shows good affinity with biopolymer [33]. PEG modification on MWCNTs reduced the nonspecific adsorption of protein as well as enhanced the water dispersing ability of MWCNTs. Besides, parts of the ferromagnetic catalyst residues were retained in the MWCNTs during synthesis and made it convenient for further purification by magnetic separation. It is determined that the strategy of incorporating antibody, the fluorescent component, as well as PEG in the magnetic MWCNTs system showed high affinity toward Va, which leads to fast detection with high sensitivity. The designed platform is expected to detect the pathogen Va in real fishery food and environmental samples.

## 2. Materials and methods

### 2.1. Reagents and materials

MWCNTs are from Nanotech (Shenzhen Nanotech Port Co., Ltd., Shenzhen, China). The Taq DNA polymerase, dNTP, 100 bp DNA marker are purchased from Tiangen (Tiangen Biotechnology Company, Beijing, China). 16S rRNA gene is purchased from Sangon (Shanghai Biology Public Health and Engineering Services Ltd., Shanghai, China). Agarose is purchased from Gene Tech (Shanghai Gene Technology Technical Services Ltd. packaging, Spain). *E. coli DH5α* strain, *S. aureus* strain, *B. subtilis* strain, and *P. aeruginosa* strain were provided by College of Life Sciences, Nankai University. Va strain and specific Va antibodies (Va-Ab) were provided by Tianjin Fishery Institute. 1-Pyrenebutyric acid is purchased from Sigma (Sigma Corporation, USA). All reagents used are of at least analytical grade. Doubly de-ionized water (DDW, 18.2 MΩ cm) obtained from a WaterPro water system (Labconco Corporation, Kansas City, MO, USA) was used throughout the experiments. Double distilled water ($ddH_2O$) is prepared from DDW after sterilization.

### 2.2. Syntheses of multifunctional MWCNTs-PEG-Py-Ab

The protocol of multifunctional MWCNTs-PEG-Py-Ab synthesis is illustrated in Scheme 1. (a) The MWCNTs were suspended in

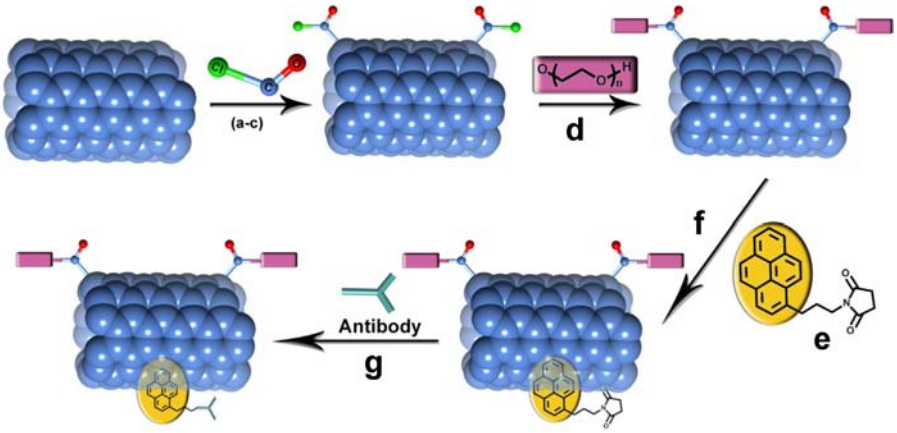


**Scheme 1.** The synthesis of multifunctional MWCNTs-PEG-Py-Ab (a) sonicated 2 h; (b) $HNO_3$, 50 °C 5 h; (c) $SOCl_2$, 70 °C 24 h; (d) $PEG_{800}$, $Et_3N$/DMF, Ar 50 °C 48 h; (e) NHS, DCC/DMF, rt, 24 h; (f) sonicated 2 h; rt, 12 h; (g) Antibody, MES, in PBS solution, rt, 10 h.

concentrated nitric acid, which was sonicated for 2 h in advance. (b) The suspension was stirred at 50 °C for 5 h and cooled to room temperature. Then, the oxidized MWCNTs (MWCNTs-COOH) were washed repeatedly with DDW until the residual acid was completely removed, and dried under vacuum. (c) The MWCNTs-COOH were dispersed in a solution of $SOCl_2$ and stirred at 70 °C for 24 h. The resultant MWCNTs-COCl were separated and dried under vacuum. (d) A mixture of $PEG_{800}$, triethylamine ($Et_3N$) in anhydrous *N*,*N*-dimethylformamide (DMF), and the MWCNT-COCl was stirred under Ar atmosphere at 50 °C for 48 h [34]. The resultant solid (MWCNT–PEG) was separated, washed with DDW and DMF sequentially, and dried under vacuum. (e) Py and *N*-hydroxysuccinimide (NHS) were dissolved in DMF. After cooling to 0 °C, 1,3-dicyclohexylcarbo-diimide (DCC) was added to the solution and the resulting mixture was stirred for 24 h. After filtration, the filtrate was collected and taken to dryness on a rotary evaporator. The resulting product was recrystallized from 95% ethanol [35]. (f) The purified product mixed with MWCNT–PEG dispersed in anhydrous DMF was sonicated for 2 h at room temperature (rt) and stirred for 12 h, then filtered through polytetrafluoroethylene membrane and washed with DDW. (g) Sufosuccimidyl CNTs phosphate-buffered saline (PBS) and Va-Ab were mixed in 2-(4-morpholino)ethanesulfonic acid (MES) buffer (pH=6.4). The mixture was shielded from light and stirred for 10 h. The resultant mixture was washed with DDW for several times, until no protein was detected in elution. Finally, the product of multifunctional MWCNTs-PEG-Py-Ab was obtained for further use.

### 2.3. Instrumentation and characterization

The morphology and microstructure of the multifunctional MWCNTs and the image of Va cells bounding to MWCNTs-PEG-Py-Ab are characterized by field-emission scanning electron microscope (SEM, FEI Nova Nano, USA). The surface morphology of several cells and the adsorption behavior of multifunctional MWCNTs are recorded with an optical microscope (XSP-C104, ChongQing Optical & Electrical Instrument Co., Ltd., China). Absorption spectra were measured with a Shimadzu UV-3600 UV–vis spectrophotometer. The FT-IR spectra (4000–400 $cm^{-1}$) in KBr were recorded using a Magna-560 spectrometer (Nicolet, Madison, WI, USA). The XRD pattern was recorded with a D/max-2500 diffractometer (Rigaku, Japan) using Cu*K*α radiation ($\lambda$=1.5418 Å). The magnetic properties of the materials were measured on a LDJ 9600-1 vibrating sample magnetometer (VSM, LDJ Electronics Inc., Troy, MI, USA). The temperature dependence of the direct current magnetic susceptibility was measured by MPMS-XL-7 (Quantum Design Magnetic Property Measurement System, USA) magnetometer. PCR was performed on TGradient Thermalblock (Whatman Biometra, Germany). The results from agarose gel electrophoresis were recorded by GDS8000 UV imager (UVtech, United Kingdom). The fluorescence measurements were performed on an F-4500 spectrofluorometer (Hitachi, Japan) equipped with a plotter unit in the fluorescence mode with excitation wavelength at 330 nm. The fluorescent spectra were recorded between 350 and 550 nm. The slit width was 10 and 10 nm for excitation and emission, respectively. The photomultiplier tube (PMT) voltage was set at 700 V.

### 2.4. Microscopic examination

*E. coli*, *S. aureus*, *B. subtilis*, *P. aeruginosa*, Va and the isolated conjugate of Va with MWCNTs-PEG-Py-Ab were visualized by crystal violet staining. After staining for about 1 min, the prepared samples were observed by optical microscope.

### 2.5. Evaluation of the selectivity of MWCNTs-PEG-Py-Ab for interactions between target and bacterial interferents by PCR reactions

To a 10 mL of 10 mg $L^{-1}$ MWCNTs-PEG-Py-Ab solution, 500 μL Va and 500 μL *E. coli* (Lane 1), 500 μL Va and 500 μL *S. aureus* (Lane 2), 500 μL Va and 500 μL *B. subtilis* (Lane 3), 500 μL Va and 500 μL *P. aeruginosa* (Lane 4) were added separately (see Fig. S1). Another equivalent amount of Va was used as a negative control (Lane 5). After incubating for about 20 min, the mixture was placed in the magnetic separator for 10 min. After that, the supernatant was carefully pipetted out. And then, the magnetic precipitates were evaluated by PCR reactions after $ddH_2O$ washing. The detailed reaction was described as follows. The PCR reaction was carried out in a total volume of 20 μL containing 1 μL template (Several conjugates were extracted from bacteria with multifunctional MWCNTs and Va was served as a negative control), 0.4 μL of Taq DNA polymerase, 2 μL Taq reaction buffer, 1.6 μL dNTP, 0.5 μL 16S rRNA upstream primer (5′-AGAGTTTGATCCTGGCTCAG-3′), 0.5 μL 16S rRNA downstream primer (5′-GGTTACCTTGTTACGACTT-3′), 14 μL $ddH_2O$. The PCR reaction was routinely performed with the following cycles: the PCR mixture was denatured at 94 °C for 4 min, followed by 29 cycles of denaturing at 94 °C for 45 s, annealing at 59 °C for 1 min, and extending at 72 °C for 1 min; after 29 cycles, the reaction was given additional extension at 72 °C for 5 min before terminating the PCR at 4 °C. The PCR product was mixed with loading buffer and resolved in 0.8% agarose gel electrophoresis. The gel was stained with ethidium bromide, and the bands were visualized under UV light equipped with a camera (GDS8000).

### 2.6. Measurement procedure

The process of the MWCNTs-PEG-Py-Ab sensor for Va detection is illustrated in Scheme 2. To a 10 mL calibrated test tube, we sequentially added 1.0 mL of 100 mg $L^{-1}$ MWCNTs-PEG-Py-Ab solution, 1.0 mL of PBS buffer (pH 7.4), and a standard Va solution with given concentration. The mixture was then diluted to aimed volume with $ddH_2O$ and mixed thoroughly. After adsorbing for about 20 min at room temperature, the mixture was placed in a magnetic separator for 10 min. The supernatant was carefully pipetted out. And then the magnetic precipitate was diluted to 1 mL with $ddH_2O$. With a series concentration of Va solution, the

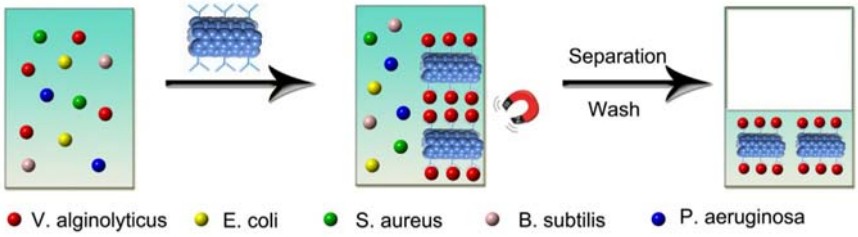


**Scheme 2.** The MWCNTs-PEG-Py-Ab based selective recognization and capturing process for Va sensing and separation.

fluorescence signal was measured with the excitation wavelength of 330 nm. The slit widths of excitation and emission were 10 and 10 nm, respectively. The emission fluorescence intensity was recorded at 402 nm (peak height).

### 2.7. Detection of Va in real samples

To evaluate the reliability of immunosensor, the MWCNTs-PEG-Py-Ab immunosensor was used to quantify Va in fishery products and fishpond water. Live shrimps purchased from a local market were washed in distilled water for several times. The finely chopped shrimp tissue was minced and homogenized in PBS buffer (weight: volume = 1:10). The mixture was filtered to remove large debris. Va was spiked into shrimp homogenate at $10^3$–$10^6$ cfu $mL^{-1}$. The inoculated homogenate was applied to test. A sample of fishpond water was also spiked with the same concentration of pathogens as described previously.

## 3. Results and discussion

### 3.1. Characterization of multifunctional MWCNTs

To confirm the formation of MWCNTs-PEG-Py-Ab conjugates, UV and FT-IR experiments were carried out. UV analysis showed that MWCNTs-PEG-Py-Ab possessed strong absorption bands at 241 nm, 272 nm and 340 nm, all of which can be ascribed to py; as well as at 280 nm which can be assigned to Va-Ab (Fig. 1a) [36]. The FT-IR spectra of MWCNTs and MWCNTs-PEG-Py-Ab, as shown in Fig. 1b, further confirmed the modification of py and Va-Ab on MWCNTs. The presence of characteristic peaks at 3330 and 645 $cm^{-1}$ for stretching vibrations of C–H may be attributed to the existence of py on the surface of MWCNTs. The final product had Va-Ab, so a secondary amide can be detected. The characteristic peaks were at 1540 $cm^{-1}$ for the deformation vibration of N–H, and at 1670 $cm^{-1}$ for the stretching vibration of C=O in –CONHR. Also PEG functionalized the surface of MWCNTs *via* ester group. Related characteristic peaks were at 1730 and 1094 $cm^{-1}$, for stretching vibrations of C=O and C–O of the ester group, respectively. In addition, the morphology study of the prepared MWCNTs-PEG-Py-Ab was monitored by SEM. The globular structures, which are well believed as Va-Ab, were observed on the wire-like MWCNTs (Fig. S2). The ferromagnetic properties of MWCNTs are mainly attributed to the catalyst nanoparticles embedded during MWCNTs synthesis through chemical vapor deposition. The embedded catalyst magnetic nanoparticles in MWCNTs are expected to be used in immuno-magnetic detection of proteins or cells [37]. The XRD spectra confirmed the existence of carbon and nickel metal (the catalyst residue) in the MWCNTs after functionalization. Graphite (0 0 2), Ni (1 1 1), Ni (2 0 0) and Ni (2 2 0) peaks from MWCNTs-PEG-Py-Ab were observed (see Fig. S3a). The magnetic properties of MWCNTs-PEG-Py-Ab prepared in the current study were evaluated using VSM. The hysteresis loops of MWCNTs-PEG-Py-Ab measured at 300 K showed ferromagnetic behavior, and their saturation magnetization (Ms) is 1.4 emu $g^{-1}$(see Fig. S3b). Fig. S3c indicated that the MWCNTs-PEG-Py-Ab contained small amounts of paramagnetic and ferromagnetic impurities. To estimate the concentration of these impurities, direct current magnetic susceptibility was measured by MPMS-XL-7 magnetometer. We obtained 11.2 ppm magnetic impurities in the MWCNTs-PEG-Py-Ab [38].

The Kjeldahl method for nitrogen determination provides quantitative analysis for the loading of Va antibody (~6.44% nitrogen) [39]. The average nitrogen content of protein is 16%, therefore 402 mg Va-Ab was immobilized onto MWCNTs per gram. The loading capability of MWCNTs for Va-Ab is much higher than that of other protein carriers. Since MWCNTs possess large specific surface area and offer more binding sites to host proteins [40–42].

### 3.2. Optimization of detection conditions

As shown in Fig. 2a, the multifunctional MWCNTs showed fluorescent emission peaks at 384 nm, 402 nm, and 423 nm, which corresponding to the py moiety attached onto MWCNTs. The fluorescent intensity of MWCNTs-PEG-Py-Ab remained stable and was not affected by time (see Fig. 2b). When binding with Va, the intensity of fluorescent emission was enhanced.

pH is an important factor in bacteria detection, also affects the properties of CNT dispersing into aqueous phase. So we further evaluated the effect of pH on enhanced fluorescent emission caused by MWCNTs-PEG-Py-Ab interacting with Va. The results indicated that the enhanced fluorescence intensity kept stable in the range of pH 6.5–7.1, increased as the pH value elevated from 7.1 to 7.4 and then leveled off as pH value changed from 8.0 to 9.0. These results revealed that the interaction between MWCNTs-PEG-Py-Ab and Va was significantly pH-dependent (see Fig. 2c). Taking both the enhanced fluorescence intensity and the bioactivities of antigen and antibody into consideration, pH 7.4 was chosen for further experiments. As in Fig. 2d, ionic strength showed no obvious influence on the enhanced fluorescence intensity, suggesting that the hydrogen bonding of antigen–antibody interaction was not affected by ionic strength in certain range. Under the optimal detection conditions, the conjugates forming could be observed. The straight rod bacteria (~2 μm) were captured by antibody functionalized MWCNTs through antibody–antigen interactions (Fig. S4).

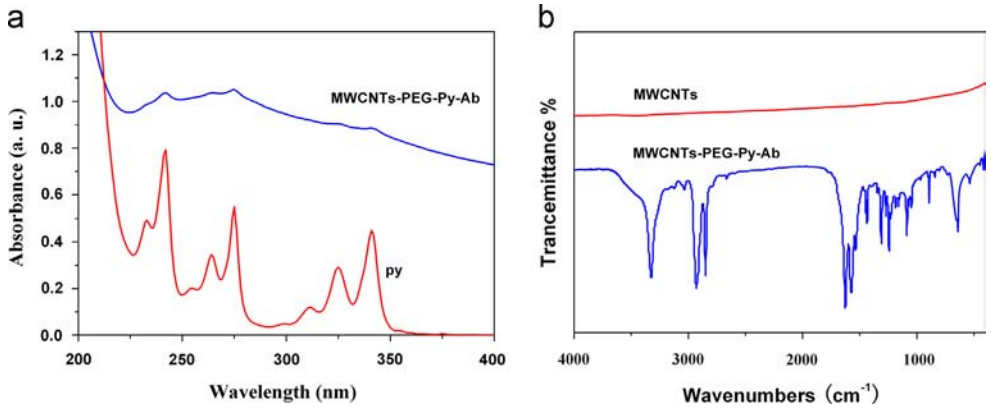


**Fig. 1.** Spectra and morphology studies toward MWCNTs-PEG-Py-Ab and its binding behavior to Va. (a) UV spectra of py and MWCNTs-PEG-Py-Ab. (b) FT-IR spectra of MWCNTs and MWCNTs-PEG-Py-Ab.

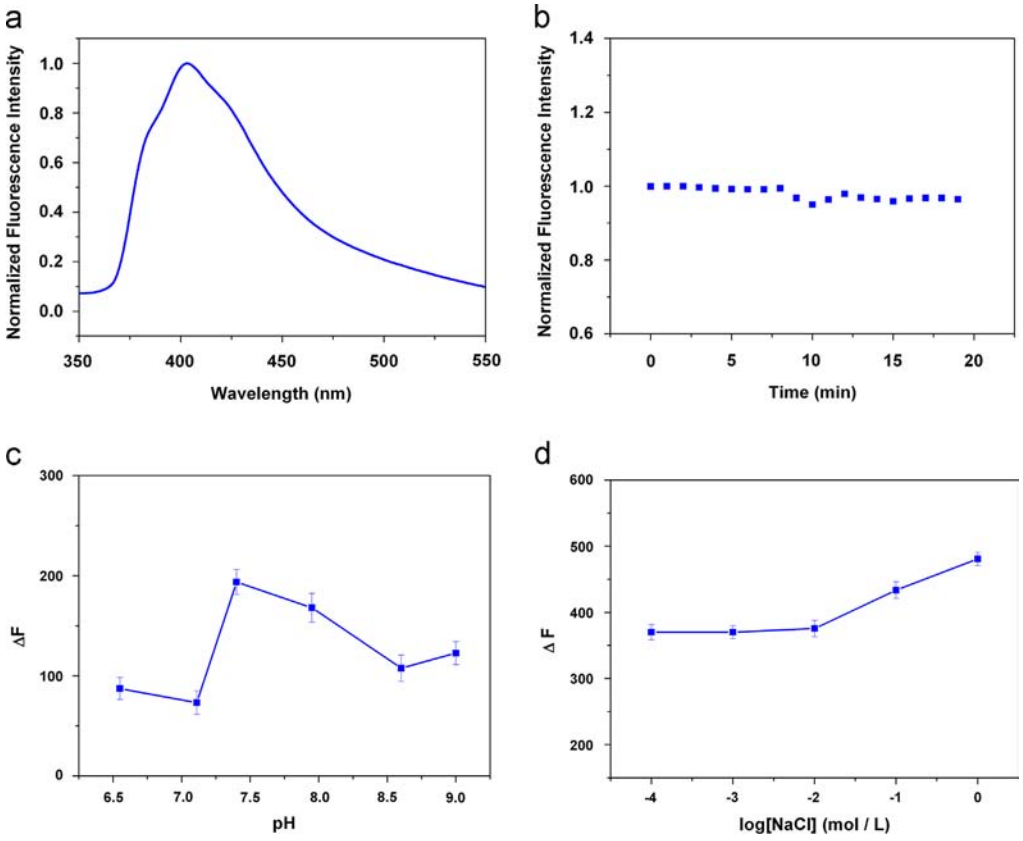


**Fig. 2.** MWCNT-PEG-Py-Ab's fluorescence properties. (a) Characterization of MWCNT-PEG-Py-Ab by fluorescent measurement. (b) Time dependent fluorescent emission of the nanohybrids MWCNTs-PEG-Py-Ab. (c) Effect of pH on the fluorescent emission of the MWCNTs-PEG-Py-Ab with Va. (d) Effect of NaCl concentration on the fluorescent emission of the nanohybrids MWCNTs-PEG-Py-Ab.

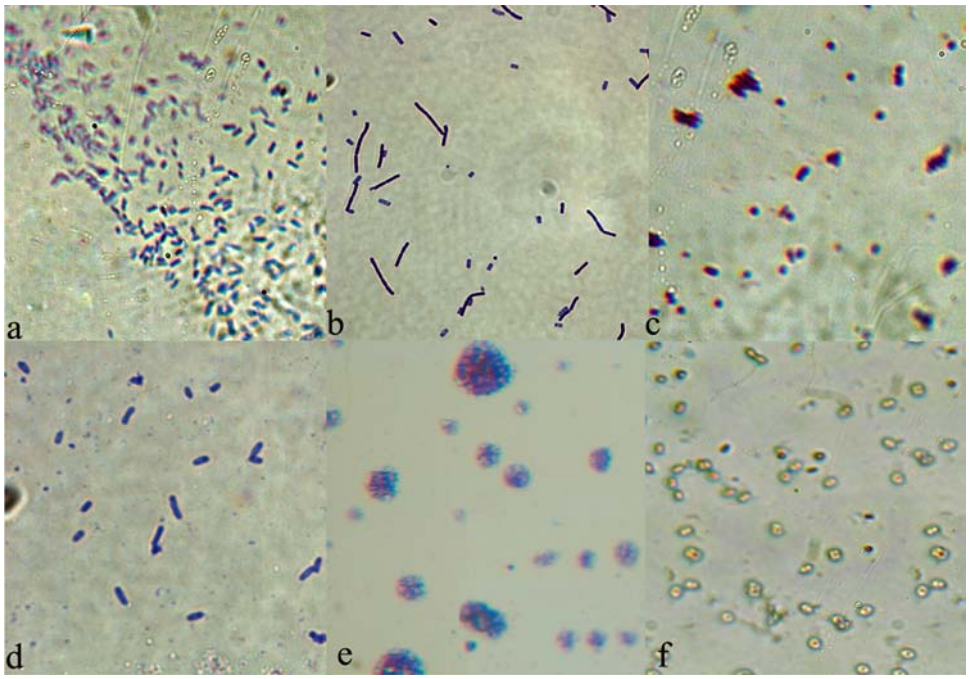


**Fig. 3.** Representative morphology profile of *E. coli* (a), *B. subtilis* (b), *S. aureus* (c), *P. aeruginosa* (d), Va (e) in the present of MWCNTs-PEG-Py-Ab, and Va (f) recorded by optical microscope.

### *3.3. Selectivity of MWCNTs-PEG-Py-Ab for Va*

We used Gram-negative bacteria, *E. coli* and *P. aeruginosa*, and Gram-positive bacteria, *S. aureu* and *B. subtilis* as interferents to assess the selectivity of the MWCNTs-PEG-Py-Ab for Va. All of the selected bacterial interferents are common pathogens in nature water and fishery products. It was assumed that the dispersing behavior of bacteria might be influenced after binding

to MWCNTs-PEG-Py-Ab because of the physical properties of MWCNTs-PEG-Py-Ab. Therefore, morphology studies were performed under optical microscope after crystal violet staining. It was found that the surface morphology of bacterial interferents was clear in the presence of MWCNTs-PEG-Py-Ab (Fig. 3a–d). As well known, *E. coli, B. subtilis, P. aeruginosa* were straight slender rods liked, and *S. aureus* was spherical shaped, all of which can be observed individually and clearly. After treated with MWCNTs-PEG-Py-Ab, none of these bacteria but Va showed changes in features. Whereas for Va, when mixed with MWCNTs-PEG-Py-Ab, only micelle-like clusters were observed (Fig. 3e) contrasting to untreated cells (Fig. 3f). It was presumed that the binding of Va with MWCNTs-PEG-Py-Ab was the main reason of cluster formation.

To further confirm the specific binding between MWCNTs-PEG-Py-Ab and Va, we used PCR reactions to detect 16S rRNA gene fragments (1500 bp) from magnetic precipitates. We first treated MWCNTs-PEG-Py-Ab with the mixture of Va and one of the other four bacterial interferents mentioned above, and then did magnetic separation. The resulting magnetic precipitates were used in PCR tests. From agarose gel electrophoresis, the 1500 bp band was observed in each of the four magnetic precipitates. Thus showed strong evidence that MWCNTs-PEG-Py-Ab and Va had specific binding, despite of the presence of bacterial interferents. Furthermore, the intensity of the 1500 bp band was the same as Va alone as negative control. This indicated that the efficiency of MWCNTs-PEG-Py-Ab capturing Va was considerably high.

### 3.4. Figures of merit for the proposed MWCNTs-PEG-Py-Ab probe based fluorescent detection of Va

The sensitivity of MWCNTs-PEG-Py-Ab as fluorescent probe for Va was investigated. The emission fluorescence intensity of the MWCNTs-PEG-Py-Ab at 402 nm was monitored to demonstrate the concentration of Va. Under the optimal conditions, the fluoresncence intensity of the MWCNTs-PEG-Py-Ab bioconjugate gradually increased as the concentration of Va elevated (Fig. 4). Enhanced fluorescence increased in a good linear relationship ($R=0.9912$) when concentrations of Va were low (from $9.0\times10^2$ to $1.5\times10^6$ cfu mL$^{-1}$). The linear regression equation was $\Delta F=7.94\times10^{-4}C+8.42$ (where $C$ stood for the concentration of Va in $10^4$ cfu mL$^{-1}$). A detection limit (3 s) of $2.8\times10^2$ cfu mL$^{-1}$ Va was achieved. The relative standard deviation (RSD) for 11 replicate detections of $1.0\times10^4$ cfu mL$^{-1}$ Va was 2.4%, which showed good precision. Till now a new immuno fluorescence assay for Va detection was preliminarily established.

Based on the above observations, the process of sensing Va using MWCNTs-PEG-Py-Ab is summarized. Since MWCNTs contain highly delocalized π electrons, the surface of MWCNTs can be easily functionalized through π−π interactions with pyrene. In this process, it is found that the photoexcited fluorophores are quenched at a certain extent by MWCNTs [43]. Va in solution gets close to and combines with the Va-Ab on the surface of MWCNTs-PEG-Py-Ab *via* the antigen–antibody interaction. When the bioconjugates MWCNTs-PEG-Py-Ab/Va formed, the quenched photoluminescence of MWCNTs-PEG-Py-Ab is highly recovered.

### 3.5. Determination of Va in shrimp and fishpond water samples

The MWCNTs-PEG-Py-Ab based fluorescent probe was applied to determine trace amount of Va in shrimp and fishpond water samples. The analysis were performed both by MWCNTs-PEG-Py-Ab immuno fluorescence assay and by commercially available ELISA method simultaneously. The reliability of the newly developed method was valued. Different combinations of bacteria were spiked and recovery analysis was pursued. As shown in Table 1, the spiked shrimps samples were tested *via* our multifunctional immunosensor assay and the recoveries and the corresponding RSD were summarized. Va recovery was in the range of 89.4–94.0% with RSD below 5.0% for the fishery samples, and in the range of 95.9–102.3% with RSD below 4.0% for the fishpond water. These data comfirmed the reliability of this newly developed immuno fluorescence assay involving MWCNTs-PEG-Py-Ab as detector.

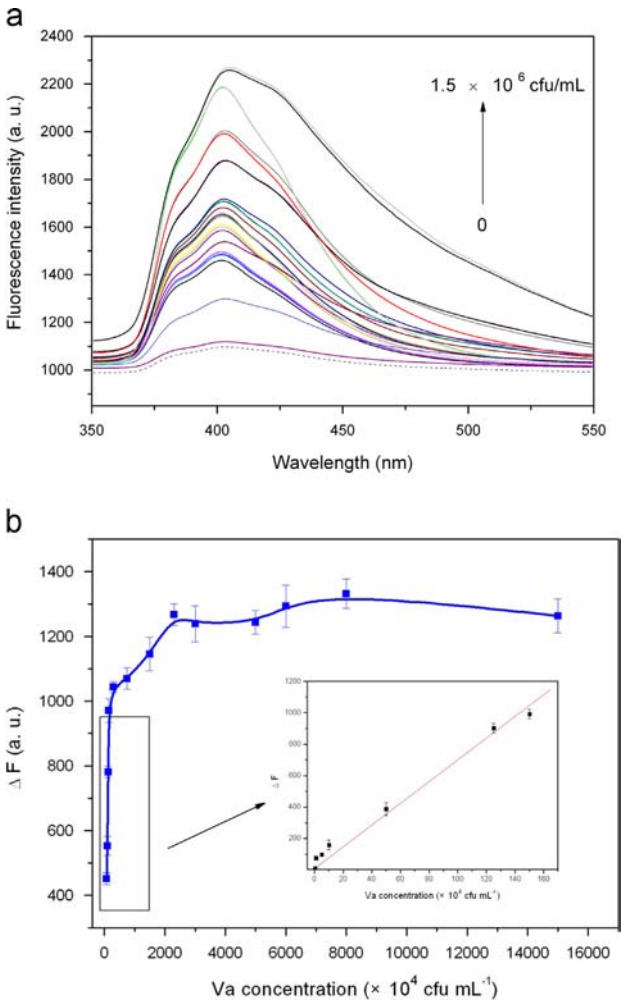


**Fig. 4.** Fluorescence analysis of MWCNTs-PEG-Py-Ab binding behavior with Va. (a) Va concentration dependent FL emission of the synthesized MWCNTs-PEG-Py-Ab. (b) Fluorescence response of MWCNT-PEG-Py-Ab to different concentrations of Va in PBS (pH=7.4) buffer.

**Table 1**
Analytical results for the determination of trace Va in real samples with the sensor in this work and ELISA method.

| Samples | Spiked (cfu mL$^{-1}$) | Magnetic-fluoresces-immuno sensor | ELISA |
|---|---|---|---|
| | | Recovery(%) (mean ± s, n=3) | Recovery(%) (mean ± s, n=3) |
| Shrimps | $10^3$ | 90.9 ± 4.1% | N/A[a] |
| | $10^4$ | 89.4 ± 2.6% | N/A[a] |
| | $10^5$ | 92.3 ± 3.5% | 86.1 ± 5.4% |
| | $10^6$ | 94.0 ± 3.8% | 92.9 ± 6.2% |
| Fishpond water | $10^3$ | 95.9 ± 3.1% | N/A[a] |
| | $10^4$ | 99.4 ± 2.7% | N/A[a] |
| | $10^5$ | 102.3 ± 2.0% | 96.8 ± 4.8% |
| | $10^6$ | 98.0 ± 1.8% | 93.5 ± 3.2% |

[a] N/A means Va is not detected.

**Table 2**
Sensitivity comparison of chemical sensor method and biological method for pathogens.

| | Detection methods | Probe | Pathogens | Detection limit (cfu $mL^{-1}$) | Refs. |
|---|---|---|---|---|---|
| Chemical sensor method | Chemiluminescent array based immunoassay | Ab-HRP array | *Escherichia coli*, *Salmonella* | $10^6$–$10^7$ | [48] |
| | Flow-through chemiluminescence microarray | Ab-HRP array | *Escherichia coli*, *Salmonella typhimurium*, *Legionella pneumophila* | $3 \times 10^6$ | [49] |
| | Immunomagnetic separation ELISA | Magnetic bead-Ab Ab-HRP | *Salmonella* | $10^5$–$10^6$ | [50] |
| | Chemiluminescent enzyme immunoassay | Ab-HRP | *Escherichia coli*, *Yersinia enterocolitica*, *Salmonella typhimurium*, *Listeria monocytogenes* | $10^4$–$10^5$ | [51] |
| | Fluorescent multianalyte array biosensor | Ab-Cy5 | *Salmonella* | $8 \times 10^4$ | [52] |
| | Cyclic voltammetry | agarose/nano–Au/Ab-HRP | *Vibrio parahaemolyticus* | $7.4 \times 10^4$ | [53] |
| | Quantum dots immunoassay | Ab-QDs | *Escherichia coli*, *Salmonella Typhimurium* | $10^4$ | [54] |
| | CNTs-based ELISA | Ab/SWCNTs/HRP | *Salmonella* | $10^4$ | [55] |
| | Electrochemical impedance spectroscopy | Ab microfabricated electrode array | *Escherichia coli* | $10^4$ | [56] |
| | Immunomagnetic separation Fluorescent biosensor | MWCNT–PEG–Py–Ab | *Vibrio alginolyticus* | $2.8 \times 10^2$ | This work |
| Biological method | Dot blot immunoassay | – | *Vibrio alginolyticus* | $10^7$–$10^8$ | [57] |
| | ELISA | – | *Vibrio alginolyticus* | $9.7 \times 10^4$ | [45] |
| | Indirect ELISA | – | *Vibrio alginolyticus* | $10^4$ | [46] |
| | Indirect ELISA | – | *Vibrio alginolyticus* | $10^4$ | [47] |
| | Loop-mediated isothermal amplification | – | *Vibrio corallilyticus* | $3.6 \times 10^4$ | [58] |
| | Real-time PCR | – | *Vibrio alginolyticus* | $10^3$ | [59] |
| | Loop-mediated isothermal amplification | – | *Vibrio alginolyticus* | $3.7 \times 10^2$ | [60] |

The results showed a good agreement between both analytical methods, indicating that MWCNTs-PEG-Py-Ab system was reliable for the simultaneous enrichment and practical for detecting viable pathogenic bacteria Va presented in fishery food and environmental samples.

### 3.6. Method comparison

When compared with widely adopted analytical methods for pathogen detection such as PCR and ELISA, this immuno fluorescence assay involving MWCNTs-PEG-Py-Ab as detector showed advantages in two aspects. On one hand, the MWCNTs-PEG-Py-Ab method was more easily carried out and therefore consumes less time. Integration of transducer and probe molecules enabled rapid and convenient measurement of Va without using any other reagent. The time required for fluorescent biosensors detection was shortened to 0.5 h, which is at least 8 h less than that of PCR–ELISA [44]. Contrast to expensive equipment used in PCR and loop-mediated isothermal amplification, fluorescent detection is a convenient, low cost and powerful technique, which has had explosive developments and applications in the field of biochemistry in recent years.

On the other hand, the sensitivity was significantly enhanced and the detection limit successfully reached $2.8 \times 10^2$ cfu $mL^{-1}$, however the detection limit of ELISA is $10^4$–$10^5$ cfu $mL^{-1}$ [45–47]. Since intake of Va contaminated fishery food or water, even at very low concentraion, could cause acute diarrhea, the sensitivity of the developed method is concerned. The comparisons between the detection method established in this research and other conventional immunological methods in literatures were summarized in Table 2. As for the conventional immuno-fluorescent technique, the detection limit is agreeable but it is difficult to avoid fussy procedures, special expensive apparatus (flow cytometry), and short-term preservation of stained specimens [61]. MWCNTs offered more stable binding sites to host antibody than ordinary polystyrene used in ELISA. During the coating process in ELISA, the antibody combination to the surface of polystyrene is mainly by hydrophobic interactions, which can be affected by the weight of antigen protein, isoelectric point, concentration, *etc.* And the coated antibody might also be washed away, thus comprise the sensitivity. In MWCNTs-PEG-Py-Ab conjugates, Va-Ab was covalently linked to py, which contributed to its high loading capability of 402 mg $g^{-1}$. The more antibodies immobilized onto MWCNTs, the more binding sites were left to Va. In the meanwhile, the bioactivity of antibody was intact. In a word, the MWCNTs presented the advantages of high capacity and enhanced stability in antigen loading. The resultant MWCNTs-PEG-Py-Ab well maintained the bioactivity of Va-Ab, and thus quantitatively analyzed Va with low detection limit [62].

## 4. Conclusions

In summary, the multifunctional MWCNTs-PEG-Py-Ab were designed for highly sensitive detection of Va. Comparing to ELISA, adopting this immuno fluorescence sensor achieved much lower detection limit (1000 times) and cost less analysis time (shorten from at least 8 h to 30 min). Moreover, the relative standard deviation for 11 replicate detections of $1.0 \times 10^4$ cfu $mL^{-1}$ Va was 2.4%, and no cross-reaction with the other four strains was observed, demonstrating a good acuracy and specificity for Va detection. The results encourage us to make further efforts on such studies and offer us promising insight into future development of fast quantitative detection of pathogen Va.

## Acknowledgments

This work was supported by the National Natural Science Foundation of China (Grants 21245001 and 51102180), and the Tianjin Natural Science Foundation (Grant 13JCQNJC06200). We also appreciate the kindly help from Dr. Xiao-Lu Jiang and Dr. Bai-Cheng Ma.

## Appendix A. Supporting information

Supplementary data associated with this article can be found in the online version at http://dx.doi.org/10.1016/j.talanta.2014.04.048.

## References


[1] Q. Chen, Q.P. Yan, S. Ma, Mar. Sci. 30 (2006) 38–98.
[2] M.C. Balebona, M.J. Andreu, M.A. Bordas, I. Zorrilla, M.A. Morinigo, J.J. Borrego, Appl. Environ. Microbiol. 64 (1998) 4269–4275.
[3] P.C. Liu, J.Y. Lin, P.T. Hsiao, K.K. Lee, J. Basic Microbiol. 44 (2004) 23–28.
[4] K.K. Lee, S.R. Yu, T.I. Yang, P.C. Liu, F.R. Chen, Lett. Appl. Microbiol. 22 (1996) 111–114.
[5] Y. Zhao, M.Q. Ye, Q.G. Chao, N.Q. Jia, Y. Ge, H.B. Shen, J. Agric. Food Chem. 57 (2009) 517–524.
[6] S. Iijima, Nature 354 (1991) 56–58.
[7] S. Niyogi, M.A. Hamon, H. Hu, B. Zhao, P. Bhowmik, R. Sen, M.E. Itkis, R.C. Haddon, Acc. Chem. Res. 35 (2002) 1105–1113.
[8] L.M. Dai, A.W.H. Mau, Adv. Mater. 13 (2001) 899–913.
[9] F.S. Lu, L.R. Gu, M.J. Meziani, X. Wang, P.G. Luo, L.M. Veca, L. Cao, Y.P. Sun, Adv. Mater. 21 (2009) 139–152.
[10] J. Lee, Y.K. Kim, D.H. Min, J. Am. Chem. Soc. 132 (2010) 14714–14717.
[11] W.J. Huang, S. Taylor, K.F. Fu, Y. Lin, D.H. Zhang, T.W. Hanks, A.M. Rao, Y.P. Sun, Nano Lett. 2 (2002) 311–314.
[12] X.W. Chen, L.L. Hu, J.W. Liu, S. Chen, J.H. Wang, TrAC, Trends Anal. Chem. 48 (2013) 30–39.
[13] H.L. Mao, N. Kawazoe, G.P. Chen, Biomaterials 34 (2013) 2472–2479.
[14] W.S.K. Nadine, H.J. Dai, J. Am. Chem. Soc. 127 (2005) 6021–6026.
[15] P. Hu, T. Tanii, G.J. Zhang, T. Hosaka, I. Ohdomari, Sens. Actuators, B: Chem. 124 (2007) 161–166.
[16] Z. Du, Y.L. Yu, X.W. Chen, J.H. Wang, Chem. Eur. J. 13 (2007) 9679–9685.
[17] X. Yu, B. Munge, V. Patel, G. Jensen, A. Bhirde, J.D. Gong, S.N. Kim, J. Gillespie, J.S. Gutkind, F. Papadimitrakopoulos, J.F. Rusling, J. Am. Chem. Soc. 128 (2006) 11199–11205.
[18] S.G. Deng, V.K.K. Upadhyayula, G.B. Smith, M.C. Mitchell, IEEE Sens. J. 8 (2008) 954–962.
[19] V.K.K. Upadhyayula, S.G. Deng, G.B. Smith, M.C. Mitchell, Water Res. 43 (2009) 148–156.
[20] T. Akasaka, F. Watari, Acta Biomater. 5 (2009) 607–612.
[21] J.Y. Lee, J.H. Jin, J.H. Kim, M.J. Kim, C.J. Lee, N.K. Min, Biotechnol. Bioeng. 109 (2012) 1471–1478.
[22] M. Hartmann, P. Betz, Y.C. Sun, S.N. Gorb, T.K. Lindhorst, A. Krueger, Chem. Eur. J. 18 (2012) 6485–6492.
[23] A.R. Deokar, L.Y. Lin, C.C. Chang, Y.C. Ling, J. Mater. Chem. B 1 (2013) 2639–2646.
[24] M.C. Gutierrez, Z.Y. Garcia-Carvajal, M.J. Hortiguela, L. Yuste, F. Rojo, M.L. Ferrer, F. del Monte, J. Mater. Chem. 17 (2007) 2992–2995.
[25] D.X. Cui, J. Nanosci. Nanotechnol. 7 (2007) 1298–1314.
[26] Y.F. Huang, Y.F. Wang, X.P. Yan, Environ. Sci. Technol. 44 (2010) 7908–7913.
[27] H.N. Abdelhamida, H.F. Wu, J. Mater. Chem. B 1 (2013) 3950–3961.
[28] Y. Lin, X.P. Jiang, T. Elkin, K.A.S. Fernando, L.R. Gu, S. Taylor, H. Yang, E. Jones, W. Wang, Y.P. Sun, J. Nanosci. Nanotechnol. 6 (2006) 868–871.
[29] A. Tiraferri, C.D. Vecitis, M. Elimelech, ACS Appl. Mater. Interfaces 3 (2011) 2869–2877.
[30] J.Y. Yuan, Y.Y. Xu, A.H.E. Muller, Chem. Soc. Rev. 40 (2011) 640–655.
[31] H.W. Rhee, C.R. Lee, S.H. Cho, M.R. Song, M. Cashel, H.E. Choy, Y.J. Seok, J.I. Hong, J. Am. Chem. Soc. 130 (2008) 784–785.
[32] C. Garcia-Aljaro, L.N. Cella, D.J. Shirale, M. Park, F.J. Munoz, M.V. Yates, A. Mulchandani, Biosens. Bioelectron. 26 (2010) 1437–1441.
[33] A. Aldalbahi, M.I.H. Panhuis, Carbon 50 (2012) 1197–1208.
[34] D.H. Jung, Y.K. Ko, H.T. Jung, Mater. Sci. Eng., C 24 (2004) 117–121.
[35] J.L. Sessler, Y. Kubo, A. Harriman, J. Phys. Org. Chem. 5 (1992) 644–648.
[36] L. Huang, D.Q. Yu, Application of UV Spectrophotometry in Organic Chemistry, Beijing Science Press, 1988.
[37] L.W. Chang, J.T. Lue, J. Nanosci. Nanotechnol. 9 (2009) 1956–1963.
[38] T. Kolodiazhnyi, M. Pumera, Small 4 (2008) 1476–1484.
[39] P.P. SaloVaananen, P.E. Koivistoinen, Food Chem. 51 (1996) 21–31.
[40] A.K. Johnson, A.M. Zawadzka, L.A. Deobald, R.L. Crawford, A.J. Paszczynski, J. Nanopart. Res. 10 (2008) 1009–1025.
[41] R. Mallik, D.S. Hage, J. Pharm. Biomed. 46 (2008) 820–830.
[42] H.K. Karagulyan, V.K. Gasparyan, S.R. Decker, Appl. Biochem. Biotechnol. 146 (2008) 39–47.
[43] Z. Zhu, R.H. Yang, M.X. You, X.L. Zhang, Y.R. Wu, W.H. Tan, Anal. Bioanal. Chem. 396 (2010) 73–83.
[44] A. Di Pinto, V. Terio, P. Di Pinto, V. Colao, G. Tantillo, Lett. Appl. Microbiol. 54 (2012) 494–498.
[45] Q.P. Yan, J. Wang, Y.Q. Su, L.B. Pi, C.R. Liu, Mar. Sci. 25 (2001) 47–49.
[46] Q.S. Zhao, Z. Xu, Y.E. Chen, S. Jin, G.H. Xu, J. Shanghai Fish. Univ. 14 (2005) 248–252.
[47] M.Y. Li, W.C. Ding, J. Chen, Y.H. Shi, J. Fish. Chin. 34 (2010) 1559–1565.
[48] N. Karoonuthaisiri, R. Charlermroj, U. Uawisetwathana, P. Luxananil, K. Kirtikara, O. Gajanandana, Biosens. Bioelectron. 24 (2009) 1641–1648.
[49] A. Wolter, R. Niessner, M. Seidel, Anal. Chem. 80 (2008) 5854–5863.
[50] L.P. Mansfield, S.J. Forsythe, Lett. Appl. Microbiol. 31 (2000) 279–283.
[51] M. Magliulo, P. Simoni, M. Guardigli, E. Michelini, M. Luciani, R. Lelli, A. Roda, J. Agric. Food Chem. 55 (2007) 4933–4939.
[52] C.R. Taitt, Y.S. Shubin, R. Angel, F.S. Ligler, Appl. Environ. Microbiol. 70 (2004) 152–158.
[53] G.Y. Zhao, F.F. Xing, S.P. Deng, Electrochem. Commun. 9 (2007) 1263–1268.
[54] L. Yang, Y. Li, Analyst 131 (2006) 394–401.
[55] W. Chunglok, D.K. Wuragil, S. Oaew, M. Somasundrum, W. Surareungchai, Biosens. Bioelectron. 26 (2011) 3584–3589.
[56] S.M. Radke, E.C. Alocilja, Biosens. Bioelectron. 20 (2005) 1662–1667.
[57] P. Prompamorn, S. Longyant, C. Pengsuk, P. Sithigorngul, P. Chaivisuthangkura, World J. Microbiol. Biotechnol. 29 (2013) 721–731.
[58] G.F. Liu, J.Y. Wang, L.W. Xu, X. Ding, S.N. Zhou, Lett. Appl. Microbiol. 51 (2010) 301–307.
[59] J.J. Zhao, C. Chen, P. Luo, C.H. Ren, X. Jiang, Z. Zhao, C.Q. Hu, Mol. Cell. Probes 25 (2011) 137–141.
[60] S.H. Cai, Y.S. Lu, Z.H. Wu, J.C. Jian, B. Wang, Y.C. Huang, Lett. Appl. Microbiol. 50 (2010) 480–485.
[61] S.Y. Chen, Z.L. Mo, Y.L. Xu, P.J. Zhang, Mar. Sci. 26 (2002) 31–35.
[62] A. Vaseashta, D. Dimova-Malinovska, Sci. Technol. Adv. Mater. 6 (2005) 312–318.